Raman Spectroscopic Investigation and Coordination Behavior of the Polyimido S^{VI} Anions $[RS(NR)_3]^-$ and $[S(NR)_4]^{2-}$

Roland Fleischer, Bernhard Walfort, Axel Gbureck, Peter Scholz, Wolfgang Kiefer, and Dietmar Stalke*

Abstract: On the basis of Raman spectroscopic experiments and the computational assignment of the SN vibrations to small wavenumbers (640 – 920 cm^{-1}), the bonding in sulfur triimides is interpreted to be mainly electrostatic ($>S^{\oplus}-N^{\ominus}-$) rather than covalent ($S(=NR)_3$). The coordination of the *S*-alkyldiiminosulfonamide $[RS(NR')_3]^-$ and tetraazasulfate $[S(NR)_4]^{2-}$ to barium is elucidated. In the anions presented here the central sulfur atom adopts the oxidation state VI. They can be readily synthesized from sulfur triimides, by nucleophilic addition of organolithium species or lithium amides to the S=N formal double bond. Although three or four nitrogen donor centers are present, tripodal coordination to barium was not observed in any case. In the $[S(NtBu)_3]^{2-}$ dianion, tripodal coordination is facilitated by all *tert*-butyl groups pointing towards the lone pair of the sulfur atom, leaving all lone pairs of the nitrogen atoms pointing in the opposite direction. However, in $[(thf)_2Ba\{(NtBu)_3SMe\}_2]$ (**4**) the steric demand of the *S*-methyl group in the $[MeS(NtBu)_3]^-$ ion forces one *tert*-butyl group to the open site of the anion, and the third nitrogen atom is blocked. Within the $[S(NtBu)_4]^{2-}$ ion in $[(thf)_4Ba_2\{N(SiMe_3)_2\}_2\{(NtBu)_4S\}]$ (**7**), tripodal coordination to barium is precluded by the bent SN–*t*Bu arrangement. In the known isoelectronic complex $[Li_2\{(NtBu)_4W\}_2]$ with a linear W≡N–*t*Bu group tripodal coordination was observed.

Keywords: alkaline earth metals · lithium · Raman spectroscopy · S ligands · structure elucidation

Introduction

Polyimido polyanions containing p-block-element bridgeheads like $[RSi(NR)_3]^{3-}$,[1] $[RE(E'R'_2NR'')_3]^{3-}$ (R, R′ = H, alkyl, aryl; E, E′ = C, Si),[2] $[Sb(NR)_3]^{3-}$,[3a] $[Sb_2(NR)_4]^{2-}$,[3b] and $[E(NtBu)_3]^{2-}$ (E = Se, Te)[4] furnish a new family of ligand systems from which macromolecular architectures of mixed metal cages and clusters may be constructed.[5]

Our current interest lies in the chemistry of polyimido anions containing a sulfur bridgehead. In these anions the central sulfur atom can adopt either the oxidation state IV, as in the *S*-alkyliminosulfinamides[6] $[RS(NR')_2]^-$ and iminosulfindiamides[7] $[S(NR)_3]^{2-}$, or the oxidation state VI, as in the *S*-alkyldiiminosulfonamide $[RS(NR')_3]^-$ and tetraazasulfates[8a] $[S(NR)_4]^{2-}$. The anionic S^{IV} species are derived from sulfur diimides by addition of organolithium species or lithium amides to the formal double bond. By analogy the S^{VI} species are derived from sulfur triimides by similar nucleophilic addition reactions. However, the chemistry of sulfur triimides,[9] in contrast to the chemistry of sulfur diimides, is rather unexplored.[10] One of the reasons might be the limited synthetic access to sulfur triimides. Until recently only two reactions were known in which the sulfur triimide backbone is formed. These syntheses, starting from NSF_3[11, 12] or OSF_4,[13] are quite hazardous and/or give poor yields (≤ 23 %). In our investigations of the $[S(NR)_3]^{2-}$ ligand, we found a new, simple and quantitative route to sulfur triimides.[14] Hence, the way is opened up to prepare *S*-alkyldiiminosulfonamide and tetraazasulfate complexes and to explore their coordination behavior.

Raman spectroscopy is an important additional tool for determining structural parameters in organometallic compounds. The class of inorganic compounds that are discussed in this paper have not yet been studied conclusively by this method. Even for the starting materials, sulfurdi- and triimides,[12, 15, 16] only very few Raman spectroscopic investigations have been reported. These authors tentatively assigned only a few of the normal modes in such compounds. Therefore, at the beginning of our investigations we studied the vibrational behavior of the sulfur triimide $S(NtBu)_3$ using various Raman techniques, and assigned vibrational modes with assistance of the results from density functional theory

[*] Prof. D. Stalke, Dipl.-Chem. R. Fleischer, Cand.-Chem. B. Walfort
Institut für Anorganische Chemie der Universität Würzburg
Am Hubland, D-97074 Würzburg (Germany)
Fax: (+49) 931-888-4619
E-mail: dstalke@chemie.uni-wuerzburg.de
Prof. Dr. W. Kiefer, Dipl.-Chem. A. Gbureck, Dipl.-Chem. P. Scholz
Institut für Physikalische Chemie der Universität Würzburg
Am Hubland, D-97074 Würzburg (Germany)

  0947-6539/98/0411-2266 $ 17.50+.50/0

(DFT) calculations. The DFT method provides good results for the calculation of normal modes.[17] On the basis of these results the first Raman investigation of a dilithium tetraazasulfate complex is presented.

Alkaline earth metal chemistry has attracted the interest of both synthetic[18] and theoretical[19] chemists. Since alkaline earth metals have been shown to be a fundamental component of interesting materials, such as high-temperature superconductors, volatile and soluble complexes of these metals, required in CVD or sol-gel process, have been synthesized and examined in great number and variety. Recently the heavier alkaline earth metals were calculated to prefer multihapto bonding to delocalized electron density rather than σ bonding to localized electron density.[20] In a series of alkaline earth metal complexes this effect could be verified.[21, 22] It seems obvious to us to embark on transmetalation reactions utilizing soluble barium amides as metal sources, and to employ the $[RS(NR')_3]^-$ monoanion and the $[S(NR)_4]^{2-}$ dianion in barium coordination. Since in the lithium complex the $[RS(NR')_3]^-$ monoanion was found to chelate the metal rather than coordinate in a tripodal fashion, the question remains as to whether this effect is an intrinsic feature of the ligand or is induced by the small metal cation.

Abstract in German: *Auf der Grundlage neuer Ramanspektroskopischer Experimente mit daran anschließender DFT Zuordnung der SN Schwingungen zu viel niedrigeren Wellenzahlen (640–920 cm^{-1}) als bislang angenommen (1200 cm^{-1}) muß die S–N-Bindung in Schwefeltriimiden sicherlich vorwiegend elektrostatisch (> S$^{\oplus}$–N$^{\ominus}$–) und weniger als kovalente Doppelbindung (S(=NR)$_3$) interpretiert werden. Die Arbeit beschreibt das Koordinationsverhalten des S-Alkyldiiminosulfonamids $[RS(NR')_3]^-$ und Tetraazasulfats $[S(NR)_4]^{2-}$ zum schweren Erdalkalimetall Barium. In diesen Anionen nimmt das zentrale Schwefelatom die Oxidationsstufe VI ein. Sie sind über nucleophile Additionsreaktionen von lithiumorganischen Verbindungen oder Lithiumamiden an die formale Doppelbindung des Schwefeltriimids leicht zugänglich. Obwohl in diesen anionischen Liganden drei oder vier potentielle Stickstoff-Donorzentren vorhanden sind, wurde keinerlei tripodale Koordination zum relativ großen und weichen Bariumatom beobachtet. Beim Triazasulfit-Anion wird die tripodale Koordination ermöglicht, da das einsame Elektronenpaar des Schwefelatoms Platz genug läßt, so daß alle tert-Butyl-Gruppen zur selben Seite ausgerichtet werden können. So zeigen alle einsamen Elektronenpaare der Stickstoffatome in die entgegengesetzte Richtung und ermöglichen die Metallkoordination. Im [(thf)$_2$Ba{(NtBu)$_3$SMe}$_2$] (**4**) dagegen zwingt der sterische Anspruch der S-Methyl-Gruppe im [MeS(NtBu)$_3$]$^-$-Anion eine der tert-Butyl-Gruppen auf die offene Seite und blockiert ein Stickstoffatom, so daß das Bariumatom nur von zwei Stickstoffatomen chelatisiert wird. Die tripodale Koordination des [S(NtBu)$_4$]$^{2-}$-Anions in [(thf)$_4$Ba$_2${N(SiMe$_3$)$_2$}$_2$–{(NtBu)$_4$S}] (**7**) wird dadurch verhindert, daß die Einheit S-N-tBu am Stickstoffatom abgewinkelt ist. Im isoelektronischen [Li$_2${(NtBu)$_4$W}$_2$]-Komplex wird jedoch aufgrund der am Stickstoffatom linearen W≡N–tBu-Einheit tripodale Koordination ermöglicht.*

Results and Discussion

Raman spectroscopic investigations of sulfur triimide and tetraazasulfate: Various Raman techniques have been used. In the case of the sulfur triimide S(N*t*Bu)$_3$, the dispersive Raman technique applying a double monochromator and a CCD camera was employed to get the information from polarized measurements (solution studies) and also to obtain high-resolution spectra by low-temperature measurements. In the case of the main group metal complexes only FT-Raman studies with long-wavenumber excitation were successful, since visible-light excitation caused strong fluorescence. The FT-Raman spectra of the tetraazasulfate residue show the same relative intensities and wavenumbers as the Raman spectra obtained from excitation with visible laser lines. The information from the Raman spectrum obtained by the dispersive method of the sulfur triimide was included to discuss the FT-Raman spectrum of the tetraazasulfate [(thf)$_4$-Li$_2$(N*t*Bu)$_4$S] (**5**).

The DFT calculation gives a C_{3h}-symmetric structure of S(NMe)$_3$ (Figure 1) with 42 normal vibrations, whose irreducible representation is given by $8\,A'(Ra) + 18\,E'(Ra/IR) + 6\,A''(IR) + 10\,E''(Ra)$. The brackets indicate activities in Raman scattering and/or infrared absorption.

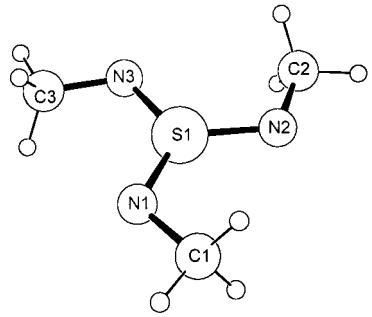

Figure 1. DFT-calulated geometry of S(NMe)$_3$, resulting in a C_{3h}-symmetric molecule; this structure is known for S(N*t*Bu)$_3$ and S(NSiMe$_3$)$_3$ from crystal-structure analyses.[24]

The sulfur triimide S(N*t*Bu)$_3$ can also be considered to have C_{3h} symmetry; in this case the methyl groups are treated as point masses. In contrast to published values[12, 15, 16] in which the SN vibrations of sulfur triimides are assigned in the region around 1200 cm^{-1} for the antisymmetric and 1150 cm^{-1} for the symmetric mode, we have located them at smaller wavenumbers, that is, in the 640–920 cm^{-1} region ($\tilde{\nu}_{asym}$-(SN$_3$) = 918 cm^{-1} and $\tilde{\nu}_{sym}$(SN$_3$) = 641 cm^{-1}). (Note: all stretching vibrations that are described in Table 3 are dominantly stretching vibrations of one bond, SN or CN; however, most of the vibrations are not pure vibrations, with only one internal coordinate involved!). This is supported by the DFT calculation of S(NMe)$_3$, in which $\tilde{\nu}_{asym}$(SN$_3$) (E′) is found at 880 cm^{-1} and $\tilde{\nu}_{sym}$(SN$_3$) at 661 cm^{-1}. Only the latter gives a polarized Raman band with very strong band at 641 cm^{-1}. For the CN-stretching vibrations, the Raman-active A′ band is calculated at 1072 cm^{-1}, whereas the experimental value of the polarized band with very strong intensity is at 1058 cm^{-1}. The calculated E′ bands (Ra/IR) at 1169/1168 cm^{-1} are assigned to the medium intensity band at 1227 cm^{-1}.

The mode at 276 cm^{-1} appears in the complex spectra with very strong intensity; this is caused by the coordinated tetrahydrofuran (THF). From this coordinated THF molecule, the high intensity of the bands at 1452 and 1215 cm^{-1} (compared with the ligand spectra) can also be rationalized (Figure 2, and Table 3 in the Experimental Section).

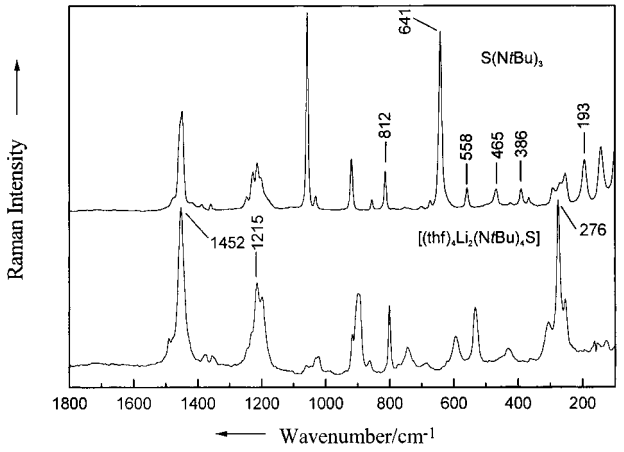

Figure 2. FT-Raman spectra of sulfurtriimide $S(NtBu)_3$ and dilithium tetraazasulfate $[(thf)_4Li_2(NtBu)_4S]$ (**5**).

***S*-methyl-*N*,*N*′,*N*″-tris(*tert*-butyl)diiminosulfonamide ($[MeS(NtBu)_3]^-$)**: *S*-alkyldiiminosulfonamides are a well established class of compounds.[23] Until recently, the only known synthetic access was the direct reaction of thiols with chloroamines or, better, bromoamines. A new synthetic route to these compounds is the nucleophilic addition of lithium alkyls to the S=N formal double bond of sulfur triimides.[8] In contrast to the chemistry of sulfur diimides, nucleophilic addition reactions in the chemistry of sulfur triimides are unfavorable due to the steric strain in the few known sulfur triimides.[24] Nevertheless, alkylation of tris(*tert*-butyl)sulfur triimide with sterically less demanding alkyls is possible.

In analogy to the synthesis of iminosulfinamides,[6] lithium methyl *N*,*N*′,*N*″-tris(*tert*-butyl)diiminosulfonamide $[(thf)_2Li_2\{(NtBu)_3SMe\}_2]$ (**1**) is obtained in the addition reaction of methyl lithium to an S=N formal double bond of $S(NtBu)_3$ [Eq. (1)].[8] A similar addition reaction with *tert*-butyl lithium failed. Presumably, the higher steric demand of the *tert*-butyl group in comparison with the methyl group prevents the nucleophilic attack at the sulfur atom. Protonation reactions of **1** were carried out, to obtain *S*-methyl *N*,*N*′,*N*″-tris(*tert*-butyl)diiminosulfonamine [Eq. (2) and (3)].

$$2\,S(NtBu)_3 + 2\,MeLi \xrightarrow{THF/hexane} [(thf)_2Li_2\{(NtBu)_3SMe\}_2]\ (\mathbf{1}) \quad (1)$$

$$2\,H_2O + [(thf)_2Li_2\{(NtBu)_3SMe\}_2] \rightarrow 2\,H(NtBu)_3SMe\ (\mathbf{2}) + 2\,LiOH \quad (2)$$

$$2\,tBuNH_3Cl + [(thf)_2Li_2\{(NtBu)_3SMe\}_2] \rightarrow 2\,H(NtBu)_3SMe\ (\mathbf{2}) + 2\,LiCl + 2\,tBuNH_2 \quad (3)$$

From the reaction of **1** with water, a yellowish oil was obtained. From this oil a colorless precipitate was formed within few hours storage at room temperature. Surprisingly, isolation of this precipitate and crystallization from pentane solution yielded pure $H(NtBu)_2SMe$ (**3**). NMR investigations of the precipitate and the residual oil revealed that the main product was $H(NtBu)_3SMe$ (**2**), with remarkable amounts of **3** as byproduct. Since **3** is a S^{IV} compound, it can not have been formed in the hydrolysis reaction itself, but must have been obtained in a subsequent redox reaction. Presumably, two $H(NtBu)_3SMe$ molecules undergo a Shenk-ene-type reaction, followed by a rearrangement accompanied by abstraction of di(*tert*-butyl)diimide, which was identified by ^1H NMR spectroscopy (Scheme 1).

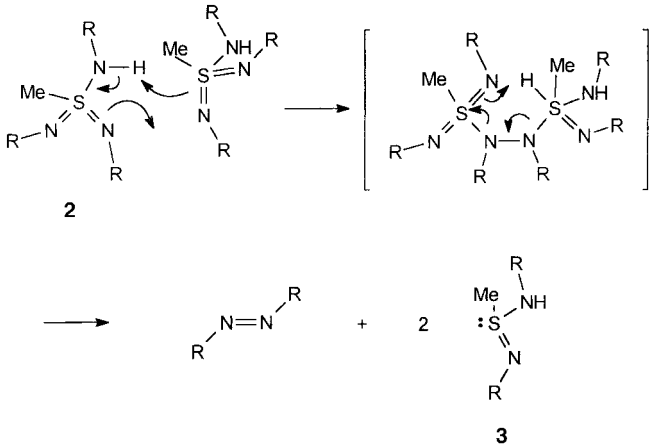

Scheme 1. Rearrangement of $H(NtBu)_3SMe$ (**2**) to give $H(NtBu)_2SMe$ (**3**).

In general, deprotonation of acidic NH functions with strong bases like the alkaline earth metal bis[bis(trimethylsilyl)amides][25] provides easy access to alkaline earth metal complexes. Hence, the reaction of **2** with $[(thf)_2Ba\{N(SiMe_3)_2\}_2]$ yields the barium complex of the $[MeS(NtBu)_3]^-$ monoanion [Eq. (4)].

$$2\,H(NtBu)_3SMe\ (\mathbf{2}) + [(thf)_2Ba\{N(SiMe_3)_2\}_2] \xrightarrow{THF/hexane} 2\,HN(SiMe_3)_2 + [(thf)_2Ba\{(NtBu)_3SMe\}_2]\ (\mathbf{4}) \quad (4)$$

***N*,*N*′,*N*″,*N*‴-Tetrakis(*tert*-butyl)tetraazasulfates ($[S(NtBu)_4]^{2-}$)**: The coordination number four is the most common for S^{VI}, and many compounds of the type $[SO_x(NR)_{4-x}]^{2-}$ or their protonated species are known.[26] Dehnicke et al. recently reported the structure of the S^{VI} dication $[S(NPMe_3)_4]^{2+}$.[27] In 1968 Appel and Ross reported the synthesis of $[K_3(HN)_3SN \cdot NH_3]$ from the reaction of *S*,*S*-dimethyl sulfur diimine with KNH_2 in liquid ammonia, which can be seen as the first member of the class of tetraazasulfates ($[S(NR)_4]^{2-}$).[28] Unfortunately it is only characterized by elemental analysis and no structural information is available. Lithium(*tert*-butyl)amide easily adds to *N*,*N*′-di(*tert*-butyl)sulfur diimide to give $[Li_4\{(NtBu)_3S\}_2]$. In a similar nucleophilic addition reaction, *N*,*N*′,*N*″-tri(*tert*-butyl)sulfur triimide yields dilithium tetrakis(*tert*-butyl)tetraazasulfate $[(thf)_4Li_2(NtBu)_4S]$ (**5**) [Eq. (5)].

$$S(NtBu)_3 + 2\,LiHNtBu \xrightarrow{THF/hexane} [(thf)_4Li_2(NtBu)_4S]\ (\mathbf{5}) + H_2NtBu \quad (5)$$

Hexane solutions of **5** form a turquoise precipitate on contact with oxygen. An ESR spectrum of the solid precipitate gave a broad signal at 3480 G without hyperfine splitting. Attempts to repeat the ESR experiment from pentane solution to obtain a better resolved spectrum have not been

0947-6539/98/0411-2268 $ 17.50+.50/0 *Chem. Eur. J.* **1998**, *4*, No. 11

successful yet. If a THF solution is exposed to oxygen, a turquoise color occurs indicating the presence of a radical species, but the color vanishes within a few seconds. The radical species is not stable in THF solution. Investigations of this oxidation reaction and its final products will follow.

In order to obtain $H_2(NtBu)_4S$ (**6**), an analogue of sulfuric acid, protonation reactions [Eq. (6) and (7)] were carried out. Unfortunately, **6** could not be isolated. On attempt to distill the crude product, it decomposed to $S(NtBu)_3$ and *tert*-butylamine. Nevertheless, in situ deprotonation of **6** with $[(thf)_2Ba\{N(SiMe_3)_2\}_2]$ gives $[(thf)_4Ba_2\{N(SiMe_3)_2\}_2\{(NtBu)_4S\}]$ (**7**) in good yield [Eq. (8)]. Even with an equimolar ratio of starting materials, a 2:1 molar ratio was found in the product.

$$2H_2O + [(thf)_4Li_2(NtBu)_4S]\ (\mathbf{5}) \rightarrow H_2(NtBu)_4S\ (\mathbf{6}) + 2LiOH \quad (6)$$

$$2tBuNH_3Cl + [(thf)_4Li_2(NtBu)_4S]\ (\mathbf{5}) \rightarrow H_2(NtBu)_4S\ (\mathbf{6}) + 2LiCl + 2tBuNH_2 \quad (7)$$

$$H_2(NtBu)_4S + 2[(thf)_2Ba\{N(SiMe_3)_2\}_2] \xrightarrow{THF/hexane} 2HN(SiMe_3)_2 + [(thf)_4Ba_2\{N(SiMe_3)_2\}_2\{(NtBu)_4S\}]\ (\mathbf{7}) \quad (8)$$

Structures of $H(NtBu)_2SMe$ (3), $[(thf)_2Ba\{(NtBu)_3SMe\}_2]$ (4) and $[(thf)_4Ba_2\{N(SiMe_3)_2\}_2\{(NtBu)_4S\}]$ (7): After one day storage at $-30\,^\circ C$ X-ray suitable crystals of **3** were obtained from a pentane solution. Like other known iminosulfinamides,[6] the solid-state structure of **3** (Figure 3) is a dimer in

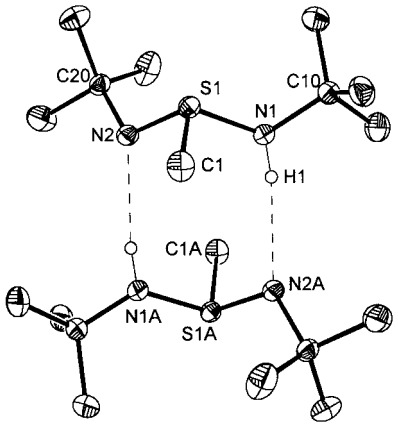

Figure 3. Solid-state structure of $H(NtBu)_2SMe$ (**3**); anisotropic displacement parameters are depicted at the 50% probability level. Selected bond lengths [pm] and angles [°]: S1–N1 168.12(12), S1–N2 158.78(11), S1–C1 179.59(14), N1–H1 84(2), H1···N2A 223(2), N1-S1-N2 109.88(6), C1-S1-N1 101.99(6), C1-S1-N2 99.79(6), S1-N1-C10 119.78(9), S1-N2-C20 114.68(9), N1-H1A···N2A 170(1).

which the two molecules are connected through weak hydrogen bridges[29] with a quite long H1···N2A (223(2) pm) distance and an N1–H1···N2A angle of 170°. Hydrogen bonding to N1 gives rise to a localized SN single bond (S1–N1: 168.1(1) pm) and a formal double bond (S1=N2: 158.8(1) pm). The S–C distance of 179.6(1) pm is comparable with the S–C distance in the $[MeS(NtBu)_3]^-$ ligand (179.7(3) pm, av).

Compound **4** crystallizes from hexane solution at room temperature within one day. The colorless blocks decompose upon heating to 250 °C. Loss of THF was not observed. In **4** the central barium atom is coordinated by two $[MeS(NtBu)_3]^-$ ligands and two additional THF molecules (Figure 4). While

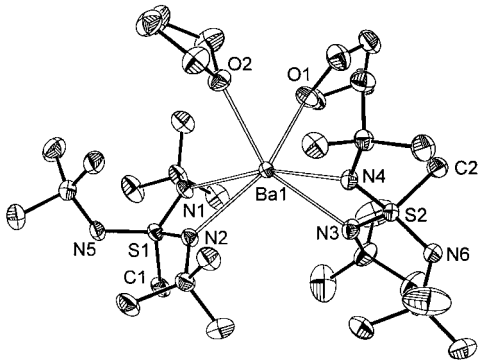

Figure 4. Solid-state structure of $[(thf)_2Ba\{(NtBu)_3SMe\}_2]$ (**4**); anisotropic displacement parameters are depicted at the 50% probability level. Selected bond lengths [pm] and angles [°]: S1–N1 157.5(2), S1–N2 157.4(2), S1–N5 154.0(2), S1–C1 179.4(3), S2–N3 157.9(2), S2–N4 157.5(2), S2–N6 153.7(2), Ba1–N1 275.9(2), Ba1–N2 267.0(2), Ba1–N3 269.8(2), Ba1–N4 276.1(2), Ba1–O1 292.2(2), Ba1–O2 278.6(2), N1-S1-N2 98.22(11), N2-S1-N5 119.93(12), N5-S1-N1 121.45(12), C1-S1-N1 109.72(13), C1-S1-N2 109.05(13), C1-S1-N5 98.30(13), N3-S2-N4 97.56(12), N4-S2-N6 121.73(13), N6-S2-N3 121.71(13), C2-S2-N3 108.76(13), C2-S2-N4 109.20(13), C2-S2-N6 97.50(13), S1-N1-C10 125.4(2), S1-N2-C20 124.4(2), S1-N5-C50 123.7(2), S2-N3-C30 125.1(2), S2-N4-C40 125.2(2), S2-N6-C60 125.8(2).

tripodal coordination of the ligand was anticipated, only two nitrogen atoms of each ligand are coordinated to the metal center. Similar to the coordination of $[PhS(NSiMe_3)_2]^-$ and $[(SiMe_3)_2NS(NSiMe_3)_2]^-$ in alkaline earth metal complexes,[22] the two ligands are coordinated to the same hemisphere of the metal, leaving the two THF donor molecules coordinated to the other. The negative charge is delocalized over the chelating SN_2 backbone, indicated by the S–N distances (av 157.7(2) pm). The uncoordinated nitrogen atom shows a much shorter S–N distance (av 153.9(2) pm), which is comparable to the S=N formal double bond in $S(NtBu)_2$ (153.2 pm), but is about 2 pm longer than in $S(NtBu)_3$ (151.5 pm). While the S–N distances of the coordinated nitrogen atoms show no significant variance, two different Ba–N distances (Ba–N1(N4): 276.0(2) and Ba–N2(N3): 268.4(2) pm, av) and different Ba–O distances (Ba–O1: 292.2(2) and Ba–O2: 278.6(2) pm) are detected. This is evidently due to steric strain. However, the Ba–N distances are in the range of related distances covered from $[(thf)_2Ba\{N(SiMe_3)_2\}_2]$[25b] (259 pm) to $[Ba\{(pz^*)_3Ge\}_2]\cdot 0.5\,dioxane$[30] ($pz^* = 3,5$-dimethylpyrazol-1-yl; Ba–N(σ): 280 and Ba–N(η): 293 and 297 pm).

A closer look at the structure reveals, that each of the *tert*-butyl groups at N1 and N4 is almost eclipsed with respect to one coordinated THF molecule (C10-N1-Ba1-O1: 14.0° and C40-N4-Ba1-O2: 4.1°). While this might be the reason for the different Ba–N distances, it does not cause the differences in the Ba–O distances. Nevertheless, these differences can be explained by considering a similar steric effect. The sulfur bonded methyl group (C2) of one ligand, is almost eclipsed with respect to the THF molecule around O1 (C2-S2-Ba1-O1: 9.2°). In the other ligand, the sulfur bonded methyl group (C1) points away from the THF molecules. In accordance to observations made earlier,[21, 22] the barium atom leaves the plane of one coordinated SN_2 unit (the SN_2 and the BaN_2 planes intersect at an angle of 164.6°) to maintain interaction with the π electron density provided by the SN_2 moiety.

Compound **7** crystallizes from THF/hexane within 12 hours, to give colorless blocks suitable for X-ray structure analysis. Crystals of **7** decompose upon heating to about 200 °C. In **7**, the central $[S(NtBu)_4]^{2-}$ ligand coordinates to two barium atoms. Each barium atom is additionally coordinated by one bis(trimethylsilyl)amide anion and two THF donor molecules, leading to a distorted trigonal bipyramidal coordination polyhedron around the barium atom (Figure 5). N1, N6, and

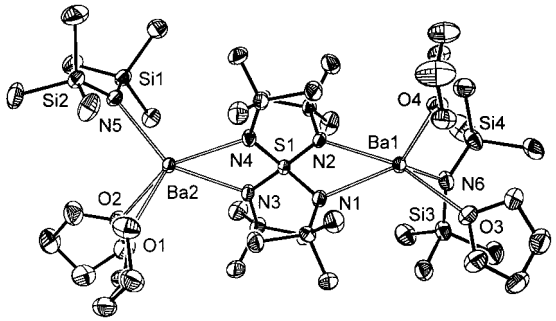

Figure 5. Solid-state structure of $[(thf)_4Ba_2\{(N(SiMe_3)_2\}_2\{(NtBu)_4S\}]$ (**7**); anisotropic displacement parameters are depicted at the 50% probability level. Selected bond lengths [pm] and angles [°]: S1–N1 160.5(3), S1–N2 159.0(3), S1–N3 159.8(3), S1–N4 159.3(3), Ba1–N1 268.2(3), Ba1–N2 266.4(3), Ba1–N6 266.5(3), Ba1–O3 283.6(3), Ba1–O4 278.1(3), Ba2–N3 268.1(3), Ba2–N4 266.4(3), Ba2–N5 266.4(3), Ba2–O1 280.3(3), Ba2–O2 285.3(3), N1-S1-N2 96.2(2), N2-S1-N3 116.2(2), N1-S1-N4 116.3(2), N2-S1-N3 116.7(2), N2-S1-N4 116.6(2), N3-S1-N4 96.3(2), S1-N1-C10 124.8(3), S1-N2-C20 125.6(3), S1-N3-C30 125.2(3), S1-N4-C40 125.7(3).

O4 (N3, N5, and O1) reside in the equatorial positions around Ba1 (Ba2), while N2 and O3 (N4 and O2) are located in the axial positions. Trigonal bipyramidal coordination usually causes an extension of the axial distances. In accordance the axial Ba–O distances (av 284.5(3) pm) are about 5 pm longer than the equatorial Ba–O distances (av 279.2(3) pm). Surprisingly, the Ba–N distances do not match this geometric model. The axial Ba–N distances (Ba1–N2, Ba2–N4, av 266.4(3) pm) are similar to two of the equatorial distances (Ba1–N5 and Ba2–N6, av 266.5(3) pm), and the other two equatorial distances are about 2 pm longer (Ba1–N1 and Ba2–N3, av 268.2(3) pm).

Structural comparison: In the solid-state structure of dimeric **1**, the coordination of the two $[MeS(NtBu)_3]^-$ ligands to the two lithium atoms is quite different (Figure 6).[8] The geometrical features affected most by asymmetric coordination are the S–N bond distances, whereas the overall geometrical

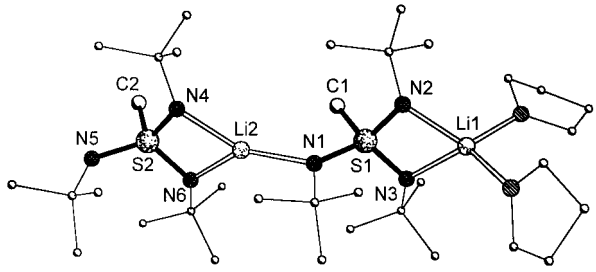

Figure 6. The structure of $[(thf)_2Li_2\{(NtBu)_3SMe\}_2]$ (**1**).

constitution differs only marginally. While coordination of both lithium atoms to one monoanion has the effect that the S–N distances in that ligand (S1 in Figure 6) are all similar (156.4(2) pm; Table 1), the S–N bond to the uncoordinated nitrogen atom (S2–N5 153.5(3) pm) is significantly shorter than the two S–N(Li) bonds (av 157.0(3) pm). The same

Table 1. Structural parameters of $[MeS(NtBu)_3]^-$; average bond lengths [pm] and angles [°]

	1 (M = Li)		**4** (M = Ba)
	S1	S2	S1 and S2
S–N(M)	156.4(2)	157.8(2)	157.7(2)
S=N		153.5(3)	153.9(2)
S–C	179.6(3)	179.9(3)	179.5(3)
(M)N–S–N(M)	97.6(1)	97.2(1)	97.9(1)
N=S–N(M)	120.1(1)	121.4(1)	121.2(1)
C–S–N(M)	110.8(1)	109.2(2)	109.2(1)
C–S=N	98.0(1)	98.3(2)	97.9(1)

phenomenon is observed in **4**. While the S–N bonds to the barium-coordinated nitrogen atoms are 157.7(2) on average, the two distances to the uncoordinated nitrogen atoms (N5 and N6 in Figure 4) are shorter (av 153.9(2) pm).

In both structures the tertiary carbon atoms at the SN_2 residue chelating the metal are almost in the plane of this group. This coordination mode is very similar to that observed in $[(thf)_nM\{(NSiMe_3)_2SN(SiMe_3)_2\}_2]$ (M = Mg, $n = 0$; M = Sr, $n = 1$).[21] The third *tert*-butyl group is pointing away from the *S*-methyl group to the vacant site of the anion. Due to steric crowding the *S*-methyl group is not located at the local C_3 axis, but is bent towards the nitrogen atom bearing the downwards orientated *tert*-butyl group. Tripodal coordination was not observed in either case.

In the $[S(NtBu)_3]^{2-}$ dianion, tripodal coordination is facilitated by all *tert*-butyl groups pointing towards the lone pair of the sulfur atom, leaving all lone pairs of the nitrogen atoms pointing in the opposite direction. The structure of $[Li_6\{(NtBu)_3SiMe\}_2]$ published by Veith et al.[31] shows almost rhombohedral D_{3d} symmetry, with the $\bar{3}$ axis along the Si–C bond. All *tert*-butyl groups are oriented towards the methyl group at the silicon atom. Hence all nitrogen atoms of the $[MeSi(NtBu)_3]^{3-}$ anion are exposed to lithium coordination (Figure 7a). This arrangement is suitable because the Si–N bonds are considerably longer (174 pm) than the S–N bonds in the systems reported here (157 pm). Furthermore the Si-N-C angles are wider (av 130°) than the S-N-C angles in $[MeS(NtBu)_3]^{2-}$ (120–125°). This gives the methyl group at the central silicon atom sufficient room. The repulsion to the *tert*-butyl groups, indicated by the red lenses in Figure 7, is only marginal and can by compensated by appropriate orientation of the hydrogen atoms at the methyl group. They slot into the gaps left by the *tert*-butyl groups. Such a hypothetical orientation of the *tert*-butyl groups in $[MeS(NtBu)_3]^{2-}$ is not possible due to steric crowding. The repulsion is much more pronounced than in the former example and the methyl group would not find any suitable orientation (Figure 7b). The anion minimizes steric strain by turning one *tert*-butyl group away from the methyl group

0947-6539/98/0411-2270 $ 17.50+.50/0 *Chem. Eur. J.* **1998**, *4*, No. 11

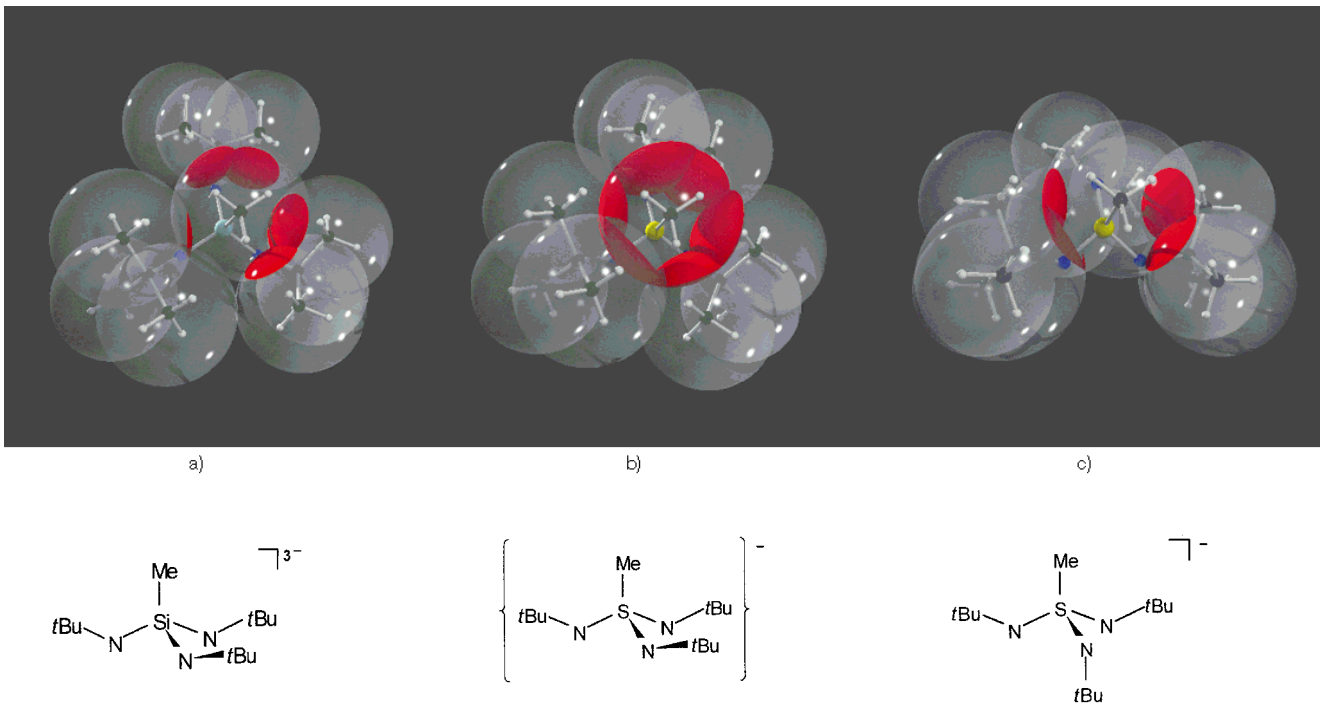

Figure 7. Space filling models[32] of a) the $[MeSi(NtBu)_3]^{3-}$ anion, b) the virtual $[MeS(NtBu)_4]^{2-}$ equivalent and c) the $[MeS(NtBu)_3]^{2-}$ conformer found in **1** and **4**. The van der Waal's radii of the methyl groups are depicted at the 200 pm level.[33] The red lenses visualize the steric overlap of the methyl group and the *tert*-butyl groups.

(Figure 7c). In this orientation, found in **1** and **4**, the steric strain is even less than in $[MeSi(NtBu)_3]^{3-}$. These findings explain why the addition reaction of *tert*-butyl lithium to sulfur triimide fails. However, the tripodal coordination is precluded because the third nitrogen atom is blocked by the sterically required orientation of the *tert*-butyl group.

Comparison of **5** and **7** reveals the geometrical features of the $[S(NtBu)_4]^{2-}$ unit (i.e., S–N distances, N-S-N angles, and C-S-N angles) to be almost invariant to the nature and coordination mode of the counterion (Table 2). Even the chelating (M)N-S-N(M) angle is only marginally affected by the different cation size in **5** and **7**. A regular tetrahedral geometry can be assumed for the separated $[S(NtBu)_4]^{2-}$ dianion, as found in SO_4^{2-}.

It is worthwhile to compare the related Group 6 metal complexes to the systems reported here.[35] While **5** is a monomer, the related complex $[Li_2\{(NtBu)_4W\}_2]$[36] shows a dimeric structure (Scheme 2), comparable with that of $[Li_4\{(NtBu)_3S\}_2]$. This structural grouping is facilitated by the linear arrangement of the uncoordinated *tert*-butylamide group, which formally requires a W≡N triple bond.

In the $[S(NR)_4]^{2-}$ anion, of course, an S≡N formal triple bond cannot be formed. An S=N formal double bond with a trigonal planar nitrogen atom would give rise to a bent geometry at nitrogen. Hence, a structural motif as found in $[Li_2\{(NtBu)_4W\}_2]$ will never be observed in the complexes of $[S(NtBu)_4]^{2-}$ owing to steric strain. In addition to the tripodal coordination pattern shown in Scheme 2a, the $[W(NtBu)_4]^{2-}$ ion (Scheme 2b) also exhibits a structural motif similar to that of the $[S(NR)_4]^{2-}$ ion.

Table 2. Structural features of $[S(NtBu)_4]^{2-}$; average bond lengths [pm] and angles [°].

	5	**7**
cation	Li^+	Ba^{2+}
cationic radii[34] [pm]	78	143
S–N	160.1(3)	159.6(3)
(M)N–S–N(M)	94.7(1)	96.3(2)
N–S–N	117.4(2)	116.5(2)
C–S–N	125.4(2)	125.3(3)

Conclusion

Some simple nucleophilic addition reactions were carried out to establish the parallels between the chemistry of sulfur diimides and sulfur triimides. The Raman spectroscopic experiments and the assignment of the SN vibrations to much

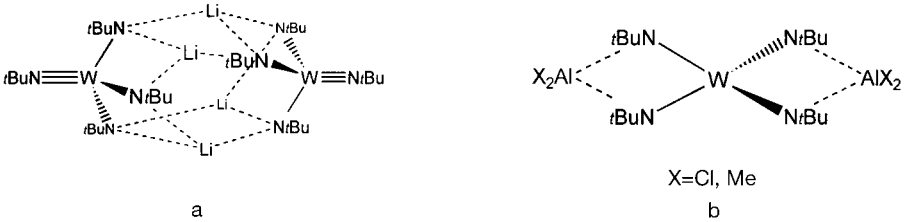

Scheme 2. Structure of a) dimeric $[Li_2\{(NtBu)_4W\}_2]$ and b) monomeric $[(AlX_2)_2\{(NtBu)_4W\}_2]$.

  0947-6539/98/0411-2271 $ 17.50+.25/0

smaller wavenumbers (640 – 920 cm^{-1}) than reported in previous papers (1200 cm^{-1}) suggest a mainly electrostatic contribution in the $>S^{\oplus}–N^{\ominus}–$ bond of sulfur triimides and related metal complexes. The hypothesis of valence expansion at sulfur to three covalent double bonds ($S(=NR)_3$) seems no longer valid. The barium metal complex of $[MeS(NtBu)_3]^-$ was structurally investigated. Contrary to our expectations, the $[MeS(NtBu)_3]^-$ ion exhibited no tripodal-coordination behavior, but only chelating properties with one N*t*Bu group remaining uncoordinated (Scheme 3). Although a third potential N-donor site is present, the coordination behavior of this monoanionic ligand resembles that of the *S*-alkyl iminosulfinamides and silylated iminosulfindiamides. The steric demand of the *S*-methyl group precludes exposure of all three nitrogen atoms to metal coordination.

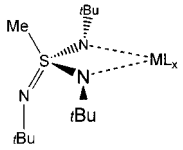

Scheme 3. Coordination behavior of $[MeS(NtBu)_3]^-$.

Although metal contact induces considerable changes in the $[MeS(NtBu)_3]^-$ ion, the $[S(NtBu)_4]^{2-}$ dianion seems to be almost invariant against the nature of the metal. The same structural motif is present in both the lithium and barium complexes (Scheme 4).

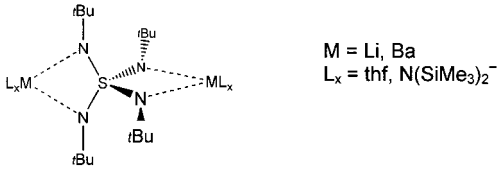

Scheme 4. Coordination behavior of $[S(NtBu)_4]^{2-}$.

Experimental Section

All manipulations were performed under inert gas atmosphere of dry N_2 with Schlenk techniques or in an argon glovebox. All solvents were dried over Na/K alloy and distilled prior to use. NMR spectra were obtained on a Bruker AM 250, Bruker MS 400, or Bruker DMX 300 at 25 °C. ESR spectra were obtained on a Bruker EPR 300 instrument at 25 °C (1 G; 100 kHz; 2 mW; 10 scans). Melting points and decomposition temperatures were measured by differential thermo analysis with a DuPont Thermal Analyzer TA 9000. Due to the high sensitivity to oxidation of most of the compounds reported here, no mass spectra are provided and no elemental analysis was attempted.

Syntheses: $[(thf)_2Li_2\{(NtBu)_3SMe\}_2]$ (**1**) and $[(thf)_4Li_2(NtBu)_4S]$ (**5**) were obtained as described previously in refs. [7] and [8a], respectively.

Synthesis of $H(NtBu)_3SMe$ (2) and $H(NtBu)_2SMe$ (3):
a) A suspension of *tert*-butylamonium chloride (4 mmol, 0.44 g) in THF (10 mL) was added to a solution of **1** (4 mmol, 2.72 g) in THF (10 mL) and stirred for 30 min. Volatile material was removed in vacuum and pentane was added to the residue. After lithium chloride was filtered off, the pentane was removed. The oily crude product was purified by fractional crystallization. Compound **2** was obtained as an amorphous white solid. $M = 261.46\ g\,mol^{-1}$; yield: 0.51 g (49 %).
b) A solution of H_2O in THF (0.5 M, 4 mmol, 8 mL) was added to a solution of **1** (4 mmol, 2.72 g) in THF (10 mL) and stirred for 30 min. Volatile material was removed under vacuum and pentane added to the residue. After lithium chloride was filtered off, the pentane was removed under vacuum. The oily crude product was purified by fractional crystallization and **2** was obtained as an amorphous white solid. Yield: 0.46 g (44 %); m.p. 86 °C; $C_{13}H_{31}N_3S$ (261.47): calcd C 59.71, H 11.95, N 16.07, S 12.26; found C 59.82, H 12.01, N 16.03, S 12.18; ^1H NMR (400 MHz, C_6D_6): $\delta = 1.28$ (s, 9H, *t*Bu), 1.29 (s, 18H, *t*Bu), 2.99 (s, 3H, CH_3).

Compound **3** crystallizes from pentane solution within 1 d storage at – 30 °C. $M = 190.34\ g\,mol^{-1}$; yield: 0.20 g (26 %); m.p. 67 °C; $C_9H_{22}N_2S$ (190.35): calcd C 56.79, H 11.65, N 14.72, S 16.84; found C 56.84, H 11.69, N 14.67, S 16.77; ^1H NMR (400 MHz, C_6D_6): $\delta = 1.26$ (s, 18H, *t*Bu), 2.93 (s, 3H, CH_3).

$[(thf)_2Ba\{(NtBu)_3SMe\}_2]$ (4): A mixture of **2** (2 mmol, 0.52 g) and barium bis[bis(trimethylsilyl)amide][25b,c] (2 mmol, 1.20 g) was dissolved in THF (10 mL) and stirred for 2 h. After all volatile material was removed under vacuum, hexane (10 mL) was added. 1 d storage at 0 °C yields colorless crystals. $M = 802.43\ g\,mol^{-1}$; yield: 1.30 g (81 %); m.p. 248 °C (decomp); ^1H NMR (300 MHz, C_6D_6): $\delta = 1.37$ (m, 4H, thf), 1.48 (s, 27H, *t*Bu), 2.83 (s, 3H, Me), 3.59 (m, 4H, thf); ^{13}C NMR (75 MHz, C_6D_6): $\delta = 25.54$ (OCH_2CH_2, thf), 33.40 (CH_3), 33.83 ($C(CH_3)_3$), 52.39 ($C(CH_3)_3$), 68.09 (OCH_2, thf).

$[(thf)_4Ba_2\{N(SiMe_3)_2\}_2\{(NtBu)_4S\}]$ (7): A suspension of *tert*-butylamonium chloride (2 mmol, 0.22 g) in THF (10 mL) was added to a solution of **5** (2 mmol, 1.24 g) in THF (10 mL), and was stirred for 30 minutes. Volatile material was removed under vacuum and pentane was added to the residue. After lithium chloride was filtered off, barium bis[bis(trimethylsilyl)amide] (2 mmol, 1.20 g) dissolved in THF (10 mL) was added and stirred for 2 hours. After all volatile material was removed under vacuum, hexane (10 mL) was added. 1 d storage at 0 °C yielded colorless crystals. $M =$ 1200.37 $g\,mol^{-1}$; yield: 1.58 g (66 %); m.p. 141 °C (decomp); ^1H NMR (400 MHz, C_6D_6): $\delta = 0.09$ (s, 36H, $SiMe_3$), 1.46 (s, 36H, *t*Bu), 1.42 (m), 3.56 (m, 16H, thf).

Raman spectroscopic experiments: For excitation of the Raman spectra the 647.1 nm line of a krypton ion laser (Spectra Physics, model 2025) was used. The scattered light was dispersed by means of a double monochromator (Spex, model 1404) and detected by a CCD (charge-coupled device) camera system (Photometrix, Spectra 9000). For solution studies a rotating quartz sample cell[37] for polarized studies was used in order to prevent local heating in the laser focus. The Raman spectra of the polycrystalline sample were recorded by means of the rotating surface-scanning technique developed by Zimmerer and Kiefer.[38] The sample was cooled at 20 K with a cryocooler (CTI-Cryogenics, model 22C). The benzene solution was prepared with absolute solvent, and all samples were handled under argon atmosphere. Sometimes the high photon energy in the visible region causes two problems: first, photochemical reactions in the laser focus are very likely, and second, fluorescence often covers the whole Raman spectrum. These two problems can be avoided with the use of excitation in the near infrared (NIR) region, for example, with a Nd:YAG laser operating at 1064 nm. The Fourier transform technique was used to compensate for two new problems: the Raman intensity is approximately proportional to the fourth power of the excitation frequency, and detectors in the near-infrared region are less sensitive. FT-Raman spectra were recorded with a Bruker spectrometer model IFS 120-HR equipped with a FT-Raman module model FRA 106. Details are given in Table 3.

DFT calculations: The DFT calculations were performed with the GAUSSIAN 94 program.[39] A combination of exchange and correlation functionals that gave the best results in test calculations was used: Becke's 1988 exchange functional[40] in combination with the Perdew-Wang 91 gradient-corrected correlation functional[41] (BPW91). The 6-31 + G* basis set for all atoms was employed in all calculations.

Crystallographic measurements: Crystal data for structures **3**, **4** and **7** are presented in Table 4. The data for all of the structures were collected at low temperatures (133(2) K) with oil-coated shock-cooled crystals[42] on a Stoe-Huber-Siemens Eigenbau diffractometer fitted with a Siemens CCD-detector and with graphite monochromated $Mo_{K\alpha}$ radiation ($\lambda =$ 0.71073 Å). Semiempirical absorption corrections were applied. The structures were solved by Patterson or direct methods with SHELXS-90.[43] All structures were refined by full-matrix least-squares procedures on F^2 with SHELXL-93.[44] All non-hydrogen atoms were refined anisotropically, and a riding model was employed in the refinement of the hydrogen atom positions. The position of the N-bound hydrogen atom H1 in **3** was taken from the difference Fourier map and refined freely, while the isotropic displacement parameter was constrained to be 1.2 times the U_{eq} of

0947-6539/98/0411-2272 $ 17.50+.50/0 *Chem. Eur. J.* **1998**, *4*, No. 11

Table 3. Calculated wavenumbers (cm^{-1}) of normal vibrations of $S(NMe)_3$ and comparison with Raman measurements of $S(NtBu)_3$ and $[(thf)_4Li_2(NtBu)_4S]$ (**5**).

$\tilde{\nu}$ [cm^{-1}] calculated $S(NMe)_3$	Assignment	$S(NtBu)_3$ (in benzene) 647.1 nm exc.	$S(NtBu)_3$ polycryst. 647.1 nm exc.	$S(NtBu)_3$ polycryst. 1064 nm exc.	**5** polycryst. 1064 nm exc.	Assignment
1467 A′ (Ra)	CH_3 out-of-phase def.	1476 vw	1481 vvw, 1473 vvw	1476 w		CH_3 out-of-phase def.
1468, 1467 E′ (Ra/IR)	CH_3 out-of-phase def.	1453 m	1457 m, 1450 m	1449 s	1452 vs (+THF)	CH_3 out-of-phase def.
1463, 1462 E″ (Ra), 1465 A″ (IR)	CH_3 out-of-phase def.	1447 m	1446 m, 1441 w			CH_3 out-of-phase def.
1169, 1168 E′ (Ra/IR)	CN stretch	1227 m	1230 m	1227 m		CN stretch
1113 A′ (Ra)	CH_3 rock	1216 m (p)	1217 m	1214 m	1215 s (+THF)	CH_3 rock [*t*Bu]
1072 A′ (Ra)	CN stretch	1058 vs (p)	1060 vvs	1057 vs	1060 w	CN stretch
1089, 1089 E″ (Ra), 1084 A″ (IR)	CH_3 rock	1031 w	1036 w, 1033 w, 1030 w	1031 w	1023 w	CH_3 rock [*t*Bu]
880 E′ (Ra/IR)	SN_3 stretch (asym.)	918 m	924 m, 922 m, 920 m, 918 m, 916 m	918 m	917 m 900 s (THF)	SN_3 stretch (asym.)
		812 m (p)	816 m	814 m	800 s	CC_3 stretch
661 A′ (Ra)	SN_3 stretch (sym.)	641 vs (p)	641 vs	642 vs	534 s	SN_3 stretch (sym.)
504, 503 E′ (Ra/IR)	SNC in plane bend	558 w	557 w	559 w		SNC in plane bend
		446 m (p)	465 w	468 w	431 w	CC_3 bend
277 A′ (Ra)	SNC in plane bend	287 m (p)	299 w, 278 w	293 w, 271 w	276 vs (+THF)	SNC in plane bend
215, 214 E″ (Ra)	SNC out of plane bend	253 m	255 m	254 m	254 m	SNC out of plane bend
		193 m (p)	194 m	194 m	164 w	CC_3 bend
144, 143 E′ (Ra/IR)	SNC in plane bend			144 m	128 w	SNC in plane bend

Table 4. Crystal data and structure refinement for **3**, **4**, and **7**.

	3	**4**	**7**
formula	$C_9H_{22}N_2S$	$C_{34}H_{76}BaN_6O_2S_2$	$C_{48}H_{112}Ba_2N_6O_5SSi_4$
M_r [g mol^{-1}]	190.35	802.47	1272.54
crystal system	monoclinic	monoclinic	triclinic
space group	$P2_1/c$	$P2_1/n$	$P\bar{1}$
a [pm]	891.92(3)	1432.83(3)	1021.47(2)
b [pm]	1482.33(6)	1728.65(3)	1779.62(2)
c [pm]	940.01(4)	1697.60(4)	1912.74(1)
α [°]	90	90	74.952(1)
β [°]	110.9823(3)	92.609(1)	80.127(1)
γ [°]	90	90	82.880(1)
V [nm^3]	1.16040(8)	4.2004(2)	3.29652(8)
Z	4	4	2
ρ_{calcd} [Mg m^{-3}]	1.090	1.269	1.282
μ [mm^{-1}]	0.237	1.079	1.333
$F(000)$	424	1704	1332
crystal size [mm]	0.8 × 0.8 × 0.7	0.4 × 0.4 × 0.3	0.7 × 0.6 × 0.1
Θ range [°]	2.70–26.40	1.85–26.49	1.82–25.03
limiting indices	$-11 \le h \le 9$	$-17 \le h \le 17$	$-11 \le h \le 12$
	$0 \le k \le 18$	$0 \le k \le 21$	$-20 \le k \le 21$
	$0 \le l \le 11$	$0 \le l \le 21$	$0 \le l \le 22$
reflections collected	6371	23446	42033
independent reflections	2277	8581	11539
R(int)	0.0190	0.0238	0.0411
data/restraints/parameters	2277/0/120	8581/304/488	11539/848/701
absorption correction	–	semiempirical	semiempirical
transmission (max./min.)	–	0.8058/0.7718	0.8988/0.6271
goodness-of-fit on F^2	1.065	1.089	1.054
$R1$ [$I > 2\sigma(I)$]	0.0315	0.0289	0.0352
$wR2$ (all data)	0.0823	0.0637	0.0867
g1/g2	0.037/0.50	0.000/6.94	0.037/5.38
largest diff. peak/hole [e nm^{-3}]	321/−304	988/−551	1014/−1440

N1. The two disordered *tert*-butyl moieties in **4** were refined to split occupancies of 0.79/0.21 (C50–C53) and 0.64/0.36 (C60–C63). In **7** the trimethylsilyl group (Si4, C64–C66) exhibits a rotational disorder; it was refined to a split occupancy of 0.61/0.39. Two coordinated THF molecules were refined to split occupancies of 0.57/0.43 (O1, C71–C74) and 0.57/0.43 (O2, C75–C78). The uncoordinated THF molecule (O1t, C91–C94) was refined to a split occupancy of 0.69/0.31. All disordered groups were refined with distance and similarity restraints. Crystallographic data (excluding structure factors) for the structures reported in this paper have been deposited with the Cambridge Crystallographic Data Centre as supplementary publication no. CCDC-101116. Copies of the data can be obtained free of charge on application to CCDC, 12 Union Road, Cambridge CB2 1EZ, UK (fax: (+44) 1223-336-033; e-mail: deposit@ccdc.cam.ac.uk).

Acknowledgments: The authors would like to thank the Deutsche Forschungsgemeinschaft (in particular SFB 347), the Fonds der Chemischen Industrie, and the Stiftung Volkswagenwerk for financial support. D.S. kindly acknowledges support of Bruker axs-Analytical X-ray Systems (Karlsruhe) and CHEMETALL (Frankfurt am Main).

Received: February 16, 1998
Revised version: June 18, 1998 [F1007]

[1] a) D. J. Brauer, H. Bürger, G. R. Liewald, J. Wilke, *J. Organomet. Chem.* **1986**, *305*, 119; b) P. Kosse, E. Popowski, M. Veith, V. Huch, *Chem. Ber.* **1994**, *127*, 2103; c) I. Hemme, U. Klingebiel, S. Freitag, D. Stalke, *Z. Anorg. Allg. Chem.* **1995**, *621*, 2093.

[2] a) H. Bürger, R. Mellies, K. Wiegel, *J. Organomet. Chem.* **1977**, *142*, 55; b) S. Friedrich, L. H. Gade, A. J. Edwards, M. McPartlin, *Chem. Ber.* **1993**, *126*, 1797; c) L. H. Gade, N. Mahr, *J. Chem. Soc. Dalton Trans.* **1993**, 489; d) K. W. Hellmann, L. H. Gade, A. Steiner, D. Stalke, F. Möller, *Angew. Chem.* **1997**, *109*, 99; *Angew. Chem. Int. Ed. Engl.* **1997**, *36*, 160; e) K. W. Hellmann, L. H. Gade, R. Fleischer, D. Stalke, *Chem. Commun.* **1997**, 527.

[3] a) R. A. Alton, D. Barr, A. J. Edwards, M. A. Paver, M.-A. Rennie, C. A. Russell, P. R. Raithby, D. S. Wright, *J. Chem. Soc. Chem. Commun.* **1994**, 1481; b) A. J. Edwards, M. A. Paver, M.-A. Rennie, C. A. Russell, P. R. Raithby, D. S. Wright, *Angew. Chem.* **1994**, *106*, 1334; *Angew. Chem. Int. Ed. Engl.* **1994**, *33*, 1277; c) M. A. Paver, C. A. Russell, D. S. Wright, *Angew. Chem.* **1995**, *107*, 1077; *Angew. Chem. Int. Ed. Engl.* **1995**, *34*, 1545; d) D. Barr, M. A. Beswick, A. J. Edwards, J. R. Galsworthy, M. A. Paver, M.-A. Rennie, C. A. Russell, P. R. Raithby, K. L. Verhorevoort, D. S. Wright, *Inorg. Chim. Acta* **1996**, *248*, 9.

[4] a) N. J. Bremer, A. B. Cutcliffe, M. F. Farona, W. G. Kofron, *J. Chem. Soc.* **1971**, 3264; b) M. Björgvinsson, H. W. Roesky, F. Pauer, G. M. Sheldrick, *Chem. Ber.* **1992**, *125*, 767; c) T. Chivers, X. Gao, M. Parvez, *Angew. Chem.* **1995**, *107*, 2756; *Angew. Chem. Int. Ed. Engl.* **1995**, *34*, 2549; d) T. Chivers, M. Parvez, G. Schatte, *Inorg. Chem.* **1996**, *35*, 4094.

[5] see for example: a) K. W. Hellmann, L. H. Gade, R. Fleischer, T. Kottke, *Chem. Eur. J.* **1997**, *3*, 1801; b) J. K. Brask, T. Chivers, M. Parvez, G. Schatte, *Angew. Chem.* **1997**, *109*, 2075; *Angew. Chem. Int. Ed. Engl.* **1997**, *36*, 1986; c) M. A. Beswick, D. S. Wright, *Coord. Chem. Rev.*, in press.

[6] a) P. Hope; L. A. Wiles, *J. Chem. Soc.* **1965**, 5386; b) O. J. Scherer, R. Schmitt, *J. Organomet. Chem.* **1969**, *16*, 11; c) O. J. Scherer, R. Wies, *Z. Naturforsch. B* **1970**, *25*, 1486; d) D. Hänssgen, W. Rölle, *J. Organomet. Chem.* **1973**, *63*, 269; e) J. Kuyper, P. C. Keijzer, K. Vrieze, *J. Organomet. Chem.* **1976**, *116*, 1; f) J. Kuyper, K. Vrieze, *J. Chem. Soc. Chem. Commun.* **1976**, 64; g) F. Pauer, D. Stalke *J. Organomet. Chem.* **1991**, *418*, 127; h) F. Pauer, J. Rocha, D. Stalke, *J. Chem. Soc. Chem. Commun.* **1991**, 1477; i) F. T. Edelmann, F. Knösel, F. Pauer, D. Stalke, W. Bauer, *J. Organomet. Chem.* **1992**, *438*, 1; k) S. Freitag, W. Kolodziejski, F. Pauer, D. Stalke *J. Chem. Soc. Dalton Trans.* **1993**, 3479.

[7] R. Fleischer, S. Freitag, F. Pauer, D. Stalke, *Angew. Chem.* **1996**, *108*, 208; *Angew. Chem. Int. Ed. Engl.* **1996**, *35*, 204.

[8] a) $[S(NR)_4]^{2-}$: R. Fleischer, A. Rothenberger, D. Stalke, *Angew. Chem.* **1997**, *109*, 1140; *Angew. Chem. Int. Ed. Engl.* **1997**, *36*, 1105; b) $S(NR)_4$: H. W. Roesky, D. P. Babb, *Angew. Chem.* **1969**, *81*, 705; *Angew. Chem. Int. Ed. Eng.* **1969**, *8*, 674.

[9] *Methoden der Organischen Chemie*, *E11*, *Parts 1 and 2* (Houben-Weyl), supplementary volume of the 4th ed., Thieme, **1985**.

[10] R. Mews, P. G. Watson, E. Lork, *Coord. Chem. Rev.* **1997**, *158*, 233.

[11] O. Glemser, J. Wegener, *Angew. Chem.* **1970**, *82*, 324; *Angew. Chem. Int. Ed. Engl.* **1970**, *9*, 309.

[12] O. Glemser, S. Pohl, F. M. Tesky, R. Mews, *Angew. Chem.* **1977**, *89*, 829; *Angew. Chem. Int. Ed. Engl.* **1977**, *16*, 789.

[13] W. Lidy, W. Sundermeyer, W. Verbeek, *Z. Anorg. Allg. Chem.* **1974**, *406*, 228.

[14] R. Fleischer, S. Freitag, D. Stalke, *J. Chem. Soc. Dalton Trans.* **1998**, 193.

[15] R. Meij, A. Oskam, D. J.Stufkens, *J. Mol. Struct.* **1979**, *51*, 37.

[16] a) A. Herbrechtsmeier, F.-M. Schnepel, O. Glemser, *J. Mol. Struct.* **1978**, *50*, 43; b) L. N. Markowskii, V. I. Tovstenko, V. E. Pashinnik, E. A. Mel'nichuk, A. G. Makarenko, Yu. G. Shermolovich, *Zh. Org. Khim.* **1991**, *27*, 769 (transl.).

[17] a) X. Zhou, C. J. M. Wheeless, R. Liu, *Vib. Spectrosc.* **1996**, *12*, 53; b) X. Zhou, R. Liu, *Vib. Spectrosc.* **1996**, *12*, 65; c) X. Zhou, S. J. Mole, R. Liu, *Vib. Spectrosc.* **1996**, *12*, 73.

[18] a) T. P. Hannusa, *Polyhedron* **1990**, *9*, 1345; b) T. P. Hannusa, *Chem. Rev.* **1993**, *93*, 1023.

[19] a) E. F. Hayes, *J. Phys. Chem.* **1966**, *70*, 3740; b) D. R. Yarkonyi, W. J. Hunt, H. F. Schaeffer, *Mol. Phys.* **1973**, *26*, 941; c) J. L. Gole, A. K. Q. Siu, E. F. Hayes, *J. Chem. Phys.* **1973**, *58*, 857; d) D. M. Hasset, C. J. Marsden, *J. Chem. Soc. Chem. Commun.* **1990**, 667; e) J. M. Dyke, T. G. Wright, *Chem. Phys. Lett.* **1990**, *169*, 138; f) L. von Szentpaly, P. Schwerdtfeger, *Chem. Phys. Lett.* **1990**, *70*, 555; g) U. Salzner, P. von R. Schleyer, *Chem. Phys. Lett.* **1990**, *172*, 461; h) R. L. DeKock, M. A. Peterson, L. K. Timmer, E. J. Baerends, P. Vernooijs, *Polyhedron* **1990**, *9*, 1919; i) L. Seijo, Z. Barandiarán, S. Huzinaga, *J. Chem. Phys.* **1991**, *94*, 3762; j) J. Kapp, P. von R. Schleyer, *Inorg. Chem.* **1996**, *35*, 2247.

[20] G. Mösges, F. Hampel, M. Kaupp, P. von R. Schleyer, *J. Am. Chem. Soc.* **1992**, *114*, 10880.

[21] R. Fleischer, D. Stalke, *Inorg. Chem.* **1997**, *36*, 2413.

[22] R. Fleischer, D. Stalke, *J. Organomet. Chem.* **1998**, *550*, 173.

[23] a) R. C. Laughlin, *Chem. Ztg.* **1968**, *92*, 383; b) R. C. Laughlin, *J. Am. Chem. Soc.* **1968**, *90*, 2651; c) R. Appel, J. Kohnke, *Chem. Ber.* **1971**, *104*, 3875; d) D. Hänsgen, W. Roelle, *J. Organomet. Chem.* **1974**, *71*, 231.

[24] a) O. Glemser, S. Pohl, F.-M. Tesky, R. Mews, *Angew. Chem.* **1977**, *89*, 829; *Angew. Chem. Int. Ed. Eng.* **1977**, *16*, 789; b) S. Pohl, B. Krebs, U. Seyer, G. Henkel, *Chem. Ber.* **1979**, *112*, 1751.

[25] a) for review see: M. Westerhausen, *Trends Organomet. Chem.* **1997**, *2*, 89; for syntheses of the Ba compound see: b) M. Westerhausen, *Inorg. Chem.* **1991**, *30*, 96; c) B. A. Vaartstra, J. C. Huffman, W. E. Streib, K. G. Caulton, *Inorg. Chem.* **1991**, *30*, 121.

[26] for example: a) R. Cramer, D. D. Cofman, *J. Org. Chem.* **1961**, *26*, 4010; b) A. J. Morris, C. H. L. Kennard, J. R. Hall, G. Smith, *Inorg. Chim. Acta* **1982**, *62*, 247; c) S. E. Kabir, M. Ruf, H. Vahrenkamp, *J. Organomet. Chem.* **1996**, *512*, 261.

[27] H. Folkerts, W. Hiller, M. Herker, S. F. Vyboishchikov, G. Frenking, K. Dehnicke, *Angew. Chem.* **1995**, *107*, 1469; *Angew. Chem. Int. Ed. Engl.* **1995**, *35*, 1362.

[28] a) R. Appel, W. Ross, *Angew. Chem.* **1968**, *80*, 561; *Angew. Chem. Int. Ed. Engl.* **1968**, *7*, 546; b) R. Appel, W. Ross, *Chem. Ber.* **1969**, *102*, 1020.

[29] a) J. Emsley, *Chem. Soc. Rev.* **1980**, *9*, 91; b) D. R. Armstrong, S. Bennet, M. G. Davidson, R. Snaith, D. Stalke, D. S. Wright, *J. Chem. Soc. Chem. Commun.* **1992**, 262; c) G. R. Desiraju, *Angew. Chem.* **1995**, *107*, 2541; *Angew. Chem. Int. Ed. Engl.* **1995**, *34*, 2328.

[30] a) A. Steiner, D. Stalke, *Inorg. Chem.* **1995**, *34*, 4846; b) T. Kottke, D. Stalke, *Chem. Ber./Rec.* **1997**, *130*, 1365.

[31] M. Veith, A. Spaniol, J. Pöhlmann, F. Gross, V. Huch, *Chem. Ber.* **1993**, *126*, 2625.

[32] a) L. Lameyer, ORT2POV, POV-Ray scene file generator; b) POV-Ray 3.0 ray tracing software, POV-Ray Team™.

[33] L. Pauling, *The Nature of the Chemical Bond*, Cornell University Press, 3rd ed., New York, **1960**, p. 261.

[34] a) J. Emsley, *The Elements*, Clarendon, Oxford, **1991**; see also b) R. D. Shannon, *Acta Crystallogr. A*, **1974**, *32*, 751.

[35] a) A. A. Danopoulos, G. Wilkinson, B. Hussain, M. B. Hursthouse, *J. Chem. Soc. Chem. Commun.* **1989**, 896; b) A. A. Danopoulos, G. Wilkinson, B. Hussain, M. B. Hursthouse, *Polyhedron* **1989**, *8*, 2947; c) A. A. Danopoulos, G. Wilkinson, B. Hussain-Bates, M. B. Hursthouse, *J. Chem. Soc. Dalton Trans.* **1990**, 2753; d) M. A. Bennett, A. A. Danopoulos, W. P. Griffith, M. L. H. Green, *J. Chem. Soc. Dalton Trans.* **1997**, 3049.

[36] a) W. A. Nugent, R. L. Harlow, *Inorg. Chem.* **1980**, *19*, 777; b) W. A. Nugent, *Inorg. Chem.* **1983**, *22*, 965.

[37] W. Kiefer, W. J. Schmid, J. A. Topp, *Appl. Spectrosc.* **1975**, *29*, 434.

[38] N. Zimmerer, W. Kiefer, *Appl. Spectrosc.* **1974**, *28*, 279.

[39] GAUSSIAN 94, Revision D.5, M. J. Frisch, G. W. Trucks, H. B. Schlegel, P. M. W. Gill, B. G. Johnson, M. A. Robb, J. R. Cheeseman, T. Keith, G. A. Petersson, J. A. Montgomery, K. Raghavachari, M. A. Al-Laham, V. G. Zakrzewski, J. V. Ortiz, J. B. Foresman, J. Cioslowski, B. B. Stefanov, A. Nanayakkara, M. Challacombe, C. Y. Peng, P. Y. Ayala, W. Chen, M. W. Wong, J. L. Andres, E. S. Replogle, R. Gomberts, R. L. Martin, D. J. Fox, J. S. Binkley, D. J. Defrees, J. Baker, J. P. Stewart, M. Head-Gordon, C. Gonzalez, J. A. Pople, Gaussian, Pittsburgh PA, **1995**.

[40] A. D. Becke, *Phys. Rev. A* **1988**, *38*, 3098.

[41] J. P. Perdew, Y. Wang, *Phys. Rev. B* **1992**, *45*, 13244.

[42] a) H. Hope, *Acta Crystallogr. B* **1988**, *44*, 22; b) T. Kottke, D. Stalke, *J. Appl. Crystallogr.* **1993**, *26*, 615; c) T. Kottke, R. J. Lagow, D. Stalke, *J. Appl. Crystallogr.* **1996**, *29*, 465.

[43] G. M. Sheldrick, *Acta Crystallogr. A* **1990**, *46*, 467.

[44] G. M. Sheldrick, *SHELXL-93, Program for Crystal Structure Refinement*, Universität Göttingen, **1996**.

0947-6539/98/0411-2274 $ 17.50+.50/0 *Chem. Eur. J.* **1998**, *4*, No. 11